https://doi.org/10.5194/nhess-2020-354
Preprint. Discussion started: 26 November 2020

Natural Hazards and Earth System Sciences
Open Access
EGU
Discussions

Long-term magnetic anomalies and its possible relationship to the latest Greater Chilean earthquakes in the context of the seismo-electromagnetic theory.

Enrique Guillermo Cordaro[1, 2], Patricio Venegas-Aravena[1, 3]and David Laroze[4].

1. Observatorios de Radiación Cósmica y Geomagnetismo. Dep. Física, F. C. F. M. Universidad de Chile, Casilla 487-3, Santiago, Chile.
2. Facultad de Ingeniería. Universidad Autónoma de Chile. Pedro de Valdivia 425. Santiago, Chile.
3. Department of Structural and Geotechnical Engineering, School of Engineering, Pontificia Universidad Católica de Chile, Vicuña Mackenna 4860, Macul, Santiago, Chile.
4. Instituto de Alta Investigación, CEDENNA, Universidad de Tarapacá, Casilla 7D, Arica, Chile.

Abstract

Several magnetic measurements and theoretical development from different research groups have shown certain relationship with worldwide geological processes. Secular variation of geomagnetic cut off rigidity, magnetic frequencies, or magnetic anomalies have been linked with spatial properties of active convergent tectonic margin or earthquakes occurrences during recent years. These include the rise of similar fundamental frequencies in the range of micro hertz before Maule 2010, Japan 2011, and Sumatra 2004 earthquakes and the dramatic rise of the cumulative number of magnetic anomalous peaks before several earthquakes as Nepal 2015 and Mexico 2017, among others. Currently, all of these measurements have been physically explained by the microcrack generation due uniaxial stress change in rock experiments. The basic physics of these experiments have been used to describe the lithospheric behavior in the context of the seismo-electromagnetic theory. Due to the dramatic increase in experimental evidence, physical mechanism and theoretical framework, this paper analyses vertical magnetic behavior close to the latest three main earthquakes in Chile: Maule 2010 (Mw8.8), Iquique 2014 (Mw8.2), and Illapel 2015 (Mw8.3). The FFT, Wavelet transform and daily cumulative number of anomalies methods were used during quiet space weather time during one year before and after each earthquake in order to filter space influence. FFT Method confirm the raise of power spectral density in mHz range before one month each earthquake, which decrease to lower values after some months after earthquake occurrence. The cumulative anomalies method exhibited and increase previous to each Chilean earthquake (50-90 days prior earthquakes) similar to those found for Nepal 2015 and Mexico 2017. The wavelet analyses also show as similar properties as FFT analysis. However, the lack of physics-based constrain in the wavelet analysis do not allow conclusion as strong as FFT and cumulative methods. By using these results and previous research, it could be stated that these magnetic features could give seismic information from impending events. Additionally, these results could be related to the Lithosphere-Atmosphere-Ionosphere coupling (LAIC effect) and the growth of micro cracks and electrification in rocks described by the seismo-electromagnetic theory.

Introduction

As earthquakes are geological events that might cause great destruction, studies about their preparation stage and generation mechanism are matter of concern. That is why scientific studies that gives new information, evidence or insights about different physical mechanism present into the seismic cycle improve our understanding of earthquakes occurrences. Currently, one of the most controversial physical mechanism that is being studied is the lithospherical electromagnetic variations as earthquake's precursory signals. Nevertheless, the study of magnetic and geological relationships is not something new. For example, the decadal variations of the geomagnetic field have been associated with an irregular flow of the outer core (Prutkin, 2008). Thus, the secular variation of the magnetic field can be interpreted as the response of the movement of the fluid outer core interacting with the topography of the lower mantle. Then, as that topography in the core-mantle boundary corresponds to a projection of the topography of the earth's surface (Soldati et al., 2012), it was not surprising that Cordaro et al. (2018) and Cordaro et al. (2019) found significant variations of geomagnetic cutoff rigidity Rc at relevant geological places in the Chilean margin.

Regarding earthquakes, many attempts to determine the location, date and magnitude of seismic movements have been made in the past (e.g. Jordan et al., 2011), but these historical efforts have failed to conclude that it is possible to use seismological data as a predictive tool (Geller, 1997). Besides, when less classical methods (e.g., electromagnetic methods) have been used some decades ago, conclusive results have not

https://doi.org/10.5194/nhess-2020-354
Preprint. Discussion started: 26 November 2020

been obtained either (see the debates of Varotsos et al. (1996) and Hough (2010)). Nevertheless, this scenario has changed during last year due the rise of more relevant and concluding evidences. For example, De Santis et al.2017, 2019, showed the method of magnetic anomalies in which long-term magnetic data from different satellites (ionosphere level) were considered during quiet or no disturbed periods due the space weather. After removing known magnetospheric process from data as daily variation, the remaining magnetic perturbation or anomaly could be considered as lithospherical origin. This method allowed them to study magnetic measurements mostly free of external perturbation prior and after 16 worldwide earthquakes of magnitude approximately greater than Mw 6.5. When satellites covered areas close to each earthquake locations, they found an increase in the number of magnetic anomalies prior (1-3 months) to the occurrence of these earthquakes and a decrease after the earthquake (De Santis et al., 2017, Marchetti and Akhoondzadeh, 2018, Marchetti et al., 2019a, b, De Santis et al., 2019).

Others methodologies also supports certain statistical correlation to earthquake's preparation phase. For instance, the rise of magnetic signals characterized by a wide range of ultra-low frequencies (5-100 mHz and 5,68 – 3.51 μHz) or the ionospheric disturbs before several earthquakes have been widely and intensively reported during a couple of decades (Hayakawa and Molchanov, 2002, Pulinets and Boyarchuk, 2004, Varotsos, 2005, Balasis and Mandea 2007, Molchanov and Hayakawa, 2008, Liu, 2009, Hayakawa et al., 2015, Contoyiannis et al., 2016, Potirakis et al., 2016, Villalobos et al., 2016, De Santis et al., 2017, Oikonomou et al., 2017, Cordaro et al., 2018, Marchetti and Akhoondzadeh, 2018, Potirakis et al., 2018, Ippolito, et al., 2020, Florios, et al., 2020, among others).

The magnetic phenomena not also have risen during decadal or preparation state, but also during the fast coseismic stage. For example, small magnetic variations (~0.8 nT) at ~100 km were measured during the Tohoku 2011 Mw9.0 earthquake (Utada et al., 2011). Similar findings were showed by Johnston et al. (2006) during Parkfield 2004 Mw6.0 earthquake (~0.3 nT) at ~2.5 km. In addition, peaks of ~0.9 nT were measured at ~7 km during Loma Prieta 1989 M7.1 earthquake (Fenoglio et al., 1995, Karakeliana et al., 2002).

The abovementioned reports have shown strong evidence of the presence of magnetic signals during the seismic preparation stage and during the rupture process itself. Up to this date, there are several experiments and theoretical models that identify and explain the physical mechanism of different magnetic variations related to geological properties (e.g. Freund, 2010, Scoville et al., 2015, Yamanaka et al., 2016, Venegas-Aravena et al., 2019, Vogel et al. 2020). According to experiments, the rise of electrical current flux within rocks is due the movement of imperfections and the suddenly growth of microcracks when rock samples are being uniaxially stressed in the semi-brittle regime (Anastasiadis et al., 2004, Stavrakas et al., 2004, Ma et al., 2011, Cartwright-Taylor et al., 2014, among others). The applied external stress generates the internal collapse of rock, which imply the fast growth of microcracks and the increase of electrical currents that flows throughout the crack right before the failure of rock samples (e.g. Triantis et al., 2008, Stavrakas et al., 2019). These currents created by this mechanism are known as pressure stimulated currents (PSC). This pre-failure indicator has been used as the experimental base for theoretical descriptions of impending earthquakes at lithospherical scale (Tzanis and Vallianatos, 2002, Vallianatos and Tzanis, 2003, Venegas-Aravena et al., 2019, Venegas-Aravena et al., 2020). This seismo-electromagnetic theory has explained the frequency range, the cumulative number of anomalies, the coseismic signals, friction states at fault, and the b-value time evolution by considering fast stress changes in the fault surrounding area. This area of fast stress changes was theorized by Dobrovolsky et al. (1979) and it could cover thousands of kilometers. Similarly, Venegas-Aravena et al. (2019) also found that the growth of microcracks and magnetic signals are hosted by these stress conditions within this large area. Recently, large areas of fast stress and strain changes, that surround the impending earthquakes, has been also confirmed by GPS analysis (Bedford et al., 2020).

Despite the abovementioned evidences, still there are no reports of cumulative anomalies in the Chilean margin. That is why this works present a wide study of magnetic signals which include spectral (Wavelet, Fourier), cumulative, and space weather analysis one year before and after the latest three main megathrust earthquakes in Chile: Maule 2010 (Mw8.8), Iquique 2014 (Mw8.2), and Illapel 2015 (Mw8.3). The space weather and general magnetic conditions are found in section 2. The main magnetic and frequency analysis are defined and performed in section 3. The relation between results and physical mechanism from the seismo-electromagnetic theory is section 4. Finally, discussions and conclusions are in section 5.

https://doi.org/10.5194/nhess-2020-354
Preprint. Discussion started: 26 November 2020

2. The space weather and magnetic conditions

2.1 External magnetic disturbances.

Before going to the study of the magnetic field and its temporal variations, it should be remembered that the rate of change of the magnetic field is influenced by the rate of variation of the spatial particle count. These are different cases of irregular and regular phenomena of the nearby space climate. Regular magnetic variation creates periodic fluctuations in the interplanetary magnetic field in a wide range of periods, from few day periods up to seasonal variations (Moldwin, 2008, Blagoveshchensky et al., 2018, Yeeram, 2019). Irregular variations occur when sudden increases of incoming solar particles are recorded across the geomagnetic field. This particle disturb induces a 10% to 20% decrease in magnetic field intensity because to the change in pressure that extraterrestrial particles exert on the magnetosphere, an effect that can last from a couple of hours to several days (Russel et al., 1999). One explication is that particles following the magnetic field lines, in the turbulent magnetic reconnection that is present in the diurnal variation and the regular variations (Priest and Forbes, 2000, Kulsrud, 2005, Cordaro, et al., 2016, Lazarian et al., 2020). Other minor irregular magnetic field as auroral events and electric current in the ionosphere are not considered for this paper (see Diego et al. (2005) for detailed description for these phenomena).

Some indexes are used in order to measure the space disturbs and its manifestation in the geomagnetic field. For example, the Kp index measure the influence of geomagnetic storms in the horizontal magnetic field (Siebert and Meyer, 1996), while Dst index is interpretated as a measure of the magnetospheric ring-current strength which is proportional to the particle's kinetic energy (e.g. Silva et al., 2017). Usually, Dst index could increase dozens or hundreds of nT during magnetic storms (Kp> 4), that is why it is important to incorporate these indexes to create reliable magnetic models.

2.2 Secular variation in the Chilean convergent margin

The magnetic response to these disturbances requires a reference model that allows to discriminate earth's magnetic features from disturbs that spreads throughout interplanetary magnetic field. One of those features corresponds to the magnetic shielding against incoming turbulent particles which is known as geomagnetic cutoff rigidity Rc (Pomerantz, 1971). The rigidity Rc is defined as the product of the force of the magnetic field and the curvature radius of the incident particle r_g and it can be estimated globally by using the Tsyganenko magnetic field model (for details see: Smart et al., 2000, Smart and Shea, 2001, Tsyganenko, 2002a, 2002b). The Rc variations describes geomagnetic secular variations which could be related to geological features in the Chilean margin (Pomerantz, 1971, Shea and Smart, 2001, Smart and Shea, 2005, Herbst et al., 2013, Cordaro et al., 2018, Cordaro et al., 2019). For example, regarding to latitudinal effect (Pomerantz, 1971), Cordaro et al. (2019) found that the highest variation rate of effective Rc values were obtained at 46.5°S, 76°W and at and at 52°S, 76.5°W (Figure 1). The first one is in the Taitao Peninsula, Chile which corresponds to the triple junction point of three tectonic plates: Nazca, South America, and Antarctica. The second one is close to Puerto Natales in the Strait of Magellan area, also a triple junction point of three tectonic plates: South America, Antarctica and Scotia (Figure 1). There are others geological and geomagnetic links as the flat slab in the Chilean convergent margin (Cordaro et al. 2018, Cordaro et al. 2019). However, these results are not surprisingly because changes in Rc represents secular variations that represents magnetic secular variations created at the outer core (Bloxham et al., 2002, McFadden and Merrill, 2007, Sarson, 2007, Finlay, 2007, Herbst et al., 2013). Specifically, 3D models of core mantle boundary (CMB) topology based on the velocities of seismic waves (Simmons et al., 2010) show the existence of positive topography in up thrust regions and negative topography in subduction zones (Yoshida, 2008, Lassak et al., 2010, Soldati et al., 2012). Let us remark that the intensity of the geomagnetic field at within the outer core it is estimated to be of the order of 2-4 mT (rms) (Olson et al., 1999, Olson, 2015), while at earth surface varies between 20,000 and 60,000 x 10^{-9} T.

The most relevant magnetic feature in the Chilean sector is the low magnetic intensity values that correspond to the influence of the South Atlantic Magnetic Anomaly (SAMA) (e.g. Cordaro et al., 2016). Recently, Tarduno et al. (2015), argued that SAMA is being created by a topography structure in the CMB beneath south Africa. SAMA is not only linked with global magnetic features as geomagnetic dipole moment (e.g. Heirtzler, 2002, Gubbins et al., 2006), it is also corresponding to the closer area between earth's surfaces and radiation belt. This proximity allows more charged particles and more disturbances in the magnetic field near the Chilean margin (e.g. Kivelson and Russell, 1995). That is why a proper magnetic response to external disturbances is required before and after earthquakes occurrences.

https://doi.org/10.5194/nhess-2020-354
Preprint. Discussion started: 26 November 2020

2.3 Magnetic perturbation during seismic events of 27/2/2010 in Maule, 1/4/2014 in Iquique and 16/9/2015 in Illapel.

The manifestation of space climate in the geomagnetic field during the periods concerned is defined by the Kp magnetic activity index as shown in Figure 2 for the months previous to the three earthquakes: Maule 2010 (Dec 12, 2009 to Mar 15, 2010), Iquique 2014 (Jan 1, 2014 to Apr 15, 2014) and Illapel 2015 (Jul 1, 2015 to Sep 30, 2015). For Maule 2010 the magnetic activity reached a Kp index equal to or greater than 4 on only three isolated occasions, it is therefore considered a calm period; for Iquique 2014, activity was concentrated around Feb 19, 2014 while for Illapel 2015 the maximum activity was recorded between September 8 and 10. In all three cases, activity did not persist in time. In fact, according to figure 2, there are no evidences of an increase in the amount of external magnetic perturbations prior each earthquake.

3 Main magnetic evolution and frequency analysis

Magnetic measurements and analysis are carried out in this section. The main aim of this section is to use different magnetic methodologies and figure out which of them seems more earthquake-related origin. The stages correspond to the long-term magnetic evolution, the simple frequency analysis, wavelet and anomaly analysis. Stations used here are Putre (PUT), Easter Island (IPM, also known as Isla de Pascua), Los Cerrillos (CER), Pilar (PIL), Osorno (OSO) and Laboratorio antártico de radiación cósmica (LARC). See Figure 1 for their location and information of PUT, CER and LARC in Table 1. In the case of PUT and IPM, the Dobrovolsky area and the earthquake distances will be used in the following subsubsections (Table 2).

3.1 **Long-term magnetic records**

A high correlation between the vertical component of the earth's magnetic field and seismic activity at the Putre station was found (Cordaro et al., 2018). That is why we seek to specify this behavior in a shorter time window than the period studied previously (1975-2010). In addition, the B_z component in Ester Island (IPM) station is also used because it has not been thoroughly investigated (Note that the IPM station was closed in 1968 and subsequently reactivated in 2008 by the French INTERMAGNET Group and the Meteorological Service of Chile) (Chulliat et al., 2009, Soloviev et al., 2012). The Putre observatory is at 18°11'47.8S, 69°33'10.9W, 3,598 m.a.s.l (meters above sea level); and it is located on the western edge of the South American Plate. This zone includes the South Atlantic Magnetic Anomaly (SAMA), the center of which is 1,700 kilometers east of this observatory. The measurements confirm low Bz values at the station Putre. The instrument error of the geomagnetic measurements is of the order of 5 nT (Cordaro et al 2012). IPM is located at 27.1°S, 109.2W, 82,83 m.a.s.l, on the western edge of the Nazca plate, characterized as a hotspot (e.g. Vezzoli and Acoocella, 2009). OSO is located in the coordinates 40°20’24” S, 74°46’64” W and PIL at 31°40’00.0” S, 63°53’00.0” W (Figure 1).

In the Putre, a diminution in the values of the whole magnetic field and each of its components is found. This can be attributed to the fact that Putre observatory is influenced by the South Atlantic Magnetic Anomaly, while on Easter Island the influence of SAMA is weaker (Storini et al., 1999). These magnetic influences are also found in Los Cerrillos observatory. The scientific and technical characteristics of the Putre (PUT) and Los Cerrillos observatories, i.e. location, altitude, atmospheric depth, type of detectors, geomagnetic cutoff rigidities and operating times, may be found in Refs. (Cordaro et al., 2012, Cordaro et al., 2016) while for Easter Island (IPM) the information is available in SuperMag Network (Chulliat et al., 2009, Gjerloev, 2012). The main characteristics for the observatories as location, altitude, atmospheric depth, type of detector, and operations time, are shown in Table 1.

Measurements of the B_z component are represented in Figure 3. We observe that similar gradients in Iquique 2014 and Illapel 2015 to those found in Maule 2010, giving rise to a jump in each case. It is known that these magnetic signals are generated by the earth's core and disseminated through the mantle, implying changes in its electrical conductivity (Stewart et al., 1995).
The jump in the B_z component for Maule 2010 was recorded in the Putre station on Jan 23, 2010 (purple solid line in Figure 3a), a time lapse of 36 days before the earthquake (solid red line) and the moment at which a change appears in the gradient or trend. It alters from a diminution of 225 nT in the period Oct 31, 2009 to Jan 23, 2010, to a less abrupt diminution of 30 nT between Jan 23, 2010 and Apr 3, 2010; prior to

Natural Hazards and Earth System Sciences
Discussions

the jump on Jan 16, 2010 there is a small, abrupt diminution from -5048 nT to -4927 nT. Discounting this small, abrupt diminution, the delta between the gradients falls from -4960 nT to -4926 nT, delta = 34 nT as it is shown in Figure 3a.

For Iquique 2014 the jump recorded in Putre (Figure 3b) occurred on Dec 27, 2013 (purple solid line), a time lapse of 96 days before the earthquake (red solid line). A change appears in the gradient on this date from a diminution of 123 nT in the period Nov 14, 2013 to Dec 27, 2013, to a diminution of 113 nT between Dec 27, 2013 and Apr 15, 2014; the jump presents a change from -7355 nT to -7235 nT, delta = 120 nT as it shown in Figure 3. For Iquique 2014 the jump measured at IPM occurred on Apr 3, 2014, a time lapse of 91 days before the earthquake (Figure 3c). The trend shows a slight increase between Sep 30, 2013 and Jan 3, 2014, from -19116 nT to -19104 nT, while a further slight increase occurs in the period Jan 3, 2014 to May 6, 2014, from -19101 nT to -19099 nT. Note that the size of the jump was -3 nT as it is shown in Figure 4. For Illapel 2015 the jump measured at IPM occurred on Aug 31, 2015, a time lapse of 16 days before the earthquake. The trend shows a slight diminution between Aug 31, 2015 and Sep 20, 2015, from -19054 nT to -19072 nT, a jump of -11 nT, as one can observe in Figure 3d.

3.2 **Simple Fourier analysis,**

Regarding the frequency analysis, the frequency spectrum values were analyzed for the Maule, Iquique and Illapel earthquakes using the second derivative of the vertical component at PUT and IPM stations. Fundamental frequencies before these earthquakes ranged from 5.606 to 3.481 µ Hertz or from 1 cycle / 48.9 hours to 1 cycle / 79.13 hours (Figure 4a). The increase in one or a group of frequencies reflects the oscillations of the radial magnetic field whose oscillation period takes from ~2 to ~4 days. Specifically, in the Maule event, peaks for the frequencies 4.747; 5.064 and 5.154 µ Hz were recorded (blue squares in Figure 4a). In Iquique peaks of 4.611; 4.882 and 5.154 µ Hz were recorded (black dots in Figure 4a), and for Illapel, 3.739; 4.630 and 5.520 µ Hz (red rhombuses in Figure 4a).

In order to identify a temporal domine where these frequencies arise, FFT is applied each 20 days as a fist approximation (Figure4b, c). Before the Iquique 2014 event a jump in intensity was observed associated with the frequency, of 5.154 µ Hz for the period Dec 27, 2013 to Jan 11, 2014, i.e. after the jump (Figure 3b, Figure 4b). Similar frequencies (3.739 µ Hz) rise during Sep 1, 2015 to Sep 8, 2015 before the Illapel 2015 event (Figure 4c). These findings imply a more detailed methodology in order to study the origin of these frequencies.

3.3 **Wavelet**

We have used the wavelet transformation to analyze localized versions of power within a geomagnetic time series, in this way it can break down a time series into the time frequency space, determine the dominant modes of variability and how they vary over time (Torrence and Compo, 1998). Here, the goal is to look for the rare variations that could not be attributed to space weather in the daily average measurements. According to Cordaro et al. (2018), the vertical component of the magnetic field showed variations related to Maule 2010 earthquake. That is why values of vertical component of the geomagnetic measurements at OSO station were considered. Note that OSO station is the closest station to the main earthquake. In order to avoid the space weather influence, highest variations where not considered. One way to perform these two restrictions, is by mean the consideration of statistical analysis. For example, a lower and upper threshold could be defined by using the standard deviation. That is, consider bigger magnetic peaks, but no to bigger because it could be related to space weather conditions. An example of this statistical analysis can be found in Figure 5 when an upper threshold of 2 standard deviation is used. There, the spectral analysis shows a dramatic increase 30 days before Maule earthquake and a decrease 10 days after the earthquake occurrence. The frequencies that rise comprise a range close to 3-5 µ Hz. Note that no other significative increase is seen during the 2 years of measurements. Despite this promise methodology, the daily average and the upper threshold, an improved implementation of the space weather, more standard anomalies and frequencies analysis is required.

3.5 **Anomaly analysis**

In order to identify and discriminate external variations from those that could be considered as lithospherical (variations with lithospherical origin), this subsection handle the definitions of anomalous variations. This definition will be obtained considering the external perturbation by using the Dst index (http://wdc.kugi.kyoto-u.ac.jp). Then, spectral analysis will be performed. Additionally, the data used in

https://doi.org/10.5194/nhess-2020-354
Preprint. Discussion started: 26 November 2020

this subsection is standard and comes from the supermag network (http://supermag.jhuapl.edu/). The data has a sampling frequency of one data per minute, and a period of one year before and one year after each earthquake was chosen.

3.5.1 **Magnetic threshold definition**

In the method for cumulative magnetic anomaly in surface of earth, we used statistically an atypical or anomalous value, that is, data that it is quite far from the average values of the sample. So, we compare real values of B_i with a more representative value of the sample, its average $B_{ave.}$ We will call the difference between the two as the magnetic residual ΔB. By using the distribution of data, we can define when a value is atypical or anomalous in a normal distribution by statistical definitions of quartiles and outliers.

First, we create a filter that eliminates the frequencies averaged near Nyquist and establishes a filter that eliminates high frequencies. The option was to consider a moving average of five points weighted: $B_{ave} = aB_{i-2} + bB_{i-1} + cB_i + bB_{i+1} + aB_{i+2}$. Here, other researchers use cubic splines instead of Moving Average (e.g. De Santis et al., 2017). In our case we use a = 0.07, b = 0.25 and c = 0.5 − 2a. The uncertainty of the Flux-gate magnetometers (supermag) used in the OSO and PIL station is $\delta B = \pm 0.1$ nT, which allows us to calculate the error propagation for averaged data $\delta B = \delta B_i + \delta B_{ave} = \pm 0.2$ nT, then the total uncertainty is $\Delta B_i + 0.2$ nT. Statistically, 0.6745σ represents 50% of the data that is closer to the average. So that 50% of the data farther from the average should be added. Then we consider as anomaly δBa all the magnetic variations that are found at an amount |δBa| of the average value. If the threshold to define the far points is 50% plus the error, then the equation to define the threshold or anomalies is $|\Delta Ba| >= 0.6745\sigma + 0.2$ nT. Where σ is the standard deviation from each record. Then, the anomalous measurements are defined by the data itself when this definition is used. The vertical magnetic thresholds are 0.2246995 nT at OSO (Feb 27, 2009 - Feb 27, 2011), 0.2362868 nT at PIL (Apr 01, 2013 – Apr 01, 2015) and 0.2352825 nT at PIL (Sep 16, 2014 – Sep 16, 2016)

Regarding the external contribution, the data considered are for quiet periods Dst <10 nT, and only quiet magnetic data between 16:00 to 05:00 local time (Hitchmn et al., 1998). Some researchers who have used satellites consider only the time periods in which the DST index is less than or equal to 20 nT (e.g. Marchetti and Akhoondzadeh, 2018), or equal to 10 nT (e.g. De Santis et al., 2017).

3.5.2 **Spectrogram**

The filtered data correspond is a strong candidacy of lithospherical magnetic origin. This mean that any spectral analysis could reveal lithospherical variations. That is why Spectrograms are performed. The spectrogram corresponds to the application of the moving Fourier transform. Here, the temporal windows size is 1 month with a 50% of overlap (see Rabiner and Schafer (1980) and Oppenheim et al. (1999) for spectrogram theory and application). The OSO and PIL spectrograms for Maule 2010, Iquique 2014 and Illapel are shown in Figure 6.

In the Maule 2010 event, the spectrogram of the vertical magnetic component at OSO station shows that the low frequency behavior around ~1-2.2 mHz appears to increase spectral density before Feb 27, 2010 (Figure 6a). Specifically, the highest frequencies appear between Jan 10, 2010 - May 02, 2010. That is more than one month before Maule earthquake. Additionally, the spectral density reduces their activity after ~2 months the earthquake. The spectrogram for Iquique 2014 is marked with two peaks, one corresponding to September 22 and the other close to March 08 (Figure 6b). The frequency range comprise between around 1.2 to 2.7 mHz. However, the main peak occurred during march with a frequency of 2.5 mHz. In Figure 6c the Illapel 2015 spectrogram is shown. Here it can be seen that almost the entire period was characterized by a close to zero frequency variations. Nevertheless, the onset of the frequency rise start closes to Aug 06, 2015 and last up to Oct 27, 2015. In the middle, a gap appears because the lost of frequency information owe strong spatial activity during September 2015. Despite this, is clear that the earthquake occurrence lies during periods of high frequency activity.

These frequency analysis shows that the three earthquakes occurred during the presence of ultra-low frequencies in the vertical magnetic component. In addition, these frequencies vanish or reduce their intensity during other time periods. Other authors have claimed that other magnetic features that accompanies ultra low frequencies is the increase of the magnetic anomalies (e.g. De Santis et al., 2017). This mean that the magnetic oscillations are produced by peaks in the magnetic records. By following the

https://doi.org/10.5194/nhess-2020-354
Preprint. Discussion started: 26 November 2020

Natural Hazards and Earth System Sciences
Discussions

Venegas-Aravena et al. (2010) findings, the number of these peaks should increase (decrease) in time before (after) earthquake occurrences.

3.5.3 **Cumulative daily anomalies**

By following the anomaly definition (subsection 3.5.1), it is possible to find out the daily number of anomalies- For example, in Figure 7 is shown the case of OSO station. Black dots follow a stable linear increase in the number of cumulative anomalies (red line). Nevertheless, this tendency breaks close to Jan 11-12, 2010. From that day up to the first weak of April, the number of anomalies experience a dramatic increase. In the middle of this increase, the Maule earthquake hit (Feb 27, 2010). By subtracting the initial linear tendency and comparing to PIL station (Iquique 2014 and Illapel 2015), the sigmoidal feature is clearer (Figure 8). The anomalies start to increase prior each earthquake. For example, this increase start ~47 days before Maule 2010 earthquake, ~90 before Iquique 2014 earthquake and ~60 days before Illapel 2015 earthquake (Figure 8).

Other researchers have used very different implementations, definitions, methodologies, and data in order to find out these anomalies. For example, Marchetti and Akhoondzadeh, (2018) have also found a sigmoidal signature in the anomalies of the Y components recorded by different satellites for the Mexico 2017 earthquake. In order to compare Mexico 2017 with Maule 2010, Iquique 2014 and Illapel 2015, the initial linear trend has been removed (Figure 9). The initial onset of anomalies increases start close to 60 day prior the Mexico 2017 earthquake. Note that in the four cases, the sigmoidal features are almost the same: a lineal stable number of anomalies characterize the initial period. Then, a dramatic increase in the number of daily anomalies is followed by the main earthquake. This time is different in each earthquake but it lies between 50 – 90 days after the initial anomalies increases. After the seismic events happens, the cumulative numbers behave not similar. For example, in the Mexico 2017 earthquake, the anomalies remain stable, while in the Maule 2010 still is increasing in a less dramatic manner. At the end of the OSO measurements, several anomalies appear, but it is not clear that these events could be related to other seismic events. In order to understand the physics that lies in these events, a theoretical mechanism is required.

4.-Magnetic anomalies and fracture mechanics by considering the seismo-electromagnetic theory.

The frequency analysis (Figure 5, 6) and cumulative number of magnetic anomalies (Figures 7, 8, 9) shows an increase (spectral intensity and anomalies number) before each earthquake occurrences. In the anomalies case, a clear sigmoidal feature rise in Maule, Iquique and Illapel, which is a similar behavior recorded in the Mexico earthquake (Figure 9, Marchetti and Akhoondzadeh, (2018)). This indicate that anomalies behavior could correspond to a lithospherical origin. Currently, it has been shown that the origin of these anomalies is associated with the cracking (or micro-cracking) of the semi-fragile-ductile part of the lithosphere (crust) due to changes in stress (Venegas-Aravena et al., 2019). Typically, strain appear when solids undergoes loads or stress accumulation. However, micro-cracks rise specifically when solids do not hold more deformation and prior the main failure (e.g. Stavrakas et al., 2019, Li et al. 2020). Experimentally, it has been shown that these conditions break the electrical neutrality within materials and generate an electrical flux through rocks in a process known as pressure stimulated currents or PSC (e.g., Anastasiadis et al., 2004). Furthermore, it has been shown that PSCs can explain that the fractal nature of cracks is sufficient to generate the frequency spectrum, co-seismic variations, the generation and behavior of anomalies, and variation in the ionosphere in a theory known as seismo-electromagnetic theory (Venegas-Aravena et al., 2019). Regarding the time evolution of magnetic anomalies, De Santis et al. (2011) have shown that the sigmoidal shape is owe to a manifestation of the stress changes when it is reaching a critical point. Nowadays, theoretical development, geodynamical measurements, and experimental studies have shown that the sigmoidal shape appears as a consequence of the dramatic increase in the number of micro cracks (at a depth of few tens of kilometers) prior the main earthquake ruptures (De Santis et al., 2015, Stavrakas et al., 2019, Venegas-Aravena, et al., 2019).

A schematical representation of the crack generation in the geodynamical context can be seen in figure 10. At the initial time $t = t_0$ the intact lithosphere undergoes a uniaxial non-constant stress σ (Figure 10a). Then the first signs of micro cracks appear at $t = t_1$ due the increase of the stress (Figure 10b). When the lithosphere can not hold more deformation, a dramatic increase in the crack generation appear throughout the lithosphere ($t = t_2$ in Figure 10c). At this point ($t = t_3$ in Figure 10d), the crack generation is no sufficient to release the excess of uniaxial stress. Then the lithosphere cannot release energy by neither deformation nor crack generation mechanism. That is why the rupture (earthquake) occurs (green area in Figure 10d) at $t = t_4$. After the main rupture, other aftershock occurs (green smaller patches within the

https://doi.org/10.5194/nhess-2020-354
Preprint. Discussion started: 26 November 2020

fault in Figure 10e). Nevertheless, the number of anomalies start to decrease. Finally, the micro crack generation stops because the deformation is sufficient to handle the lithospherical response to non-constant uniaxial stress (Figure 10f).

Additionally, Venegas-Aravena et al. (2019) found that the increase in the number of anomalies are controlled by the same fractal nature that drive the micro crack generation. This means that the frequency of the electrical flux could covers several magnitude orders. For example, figures 4, 5, and 6 are characterized for the rise of different frequencies (micro to mili Hertz), which are known as ultra-low-frequency (ULF), prior main earthquakes. These frequencies ranges were also found and described by others researches as Fenoglio et al. (1995), Vallianatos and Tzanis (2003), Fraser-Smith (2008), De Santis et al. (2017), Cordaro et al. (2018), among others.

Finally, it has been concluded that there must be precursory magnetic anomalies of the order of 0.1 nT related to earthquakes on the earth's surface (e.g. De Santis et al, 2017, Chernogor, 2019, Venegas-Aravena et al., 2019). In the previous section, it was found that the minimum value to define an anomaly was close to 0.2 nT. Therefore, this experimental result is in agreement with the theoretical value obtained. Consequently, according to the Seismo-electromagnetic theory indicates that the anomalies may have a lithospheric origin. Furthermore, the behavior of all these anomalies has a preceding increase similar to that of other seismic events that use different data and methods (e.g., De Santis et al., 2019 and references therein).

5.- Discussions and Conclusions.

The most significant characteristics of the magnetic field and its variations are found in the z-component, which we have observed and recorded at the Putre and IPM observatories. The previous measurements show that there is evidence of a progressive increase in the phenomenon known as the South Atlantic Magnetic Anomaly (SAMA) (Cordaro et al., 2019). As expected, it generates a significant deviation in the intensities present in the OP station as it is shown in the magnetic iso-values (Figure 1). Combining this information with data from the IPM station, the behavior of the radial component of the geomagnetic field for the three most significant seismic events in the Chilean Pacific sector during the period 2010-2015 was recorded, and it corroborates the magnetic relation with seismology shown in Potirakis et al. (2016), Contoyiannis et al. (2016), De Santis et al. (2017), which have been used other methods.

The normal magnetic trend showed some long-term variations. For example, there were breaks in the trend or jump of B_z, followed by a time-lapse, and seismic movement as one can observe Figure 3. These jumps occur in different forms: in Putre they are significant, reaching values of tens of nT, while in IPM the jump is barely 10nT. The time lapse between each jump and the seismic event differs in each event. For Maule 2010 it was 36 days, for Iquique 2014 it was 96 days, and for Illapel 16 days. This time difference may be due to an important factor: it appears that the jump is not equally strong in the three events, since the jump before the Iquique 2014 event was considerably. weaker than the one before Illapel 2015, and preceded the event by a longer time lapse (96 days). The more abrupt jump recorded in Illapel was followed by a shorter time lapse (16 days). These changes are notorious, that is why a first approach by using frequency analysis were done.
Specifically, significant frequencies data obtained for Maule earthquake Chile, 2010, range from 4.747 to 5.154 μ Hz, for Tohoku earthquake. Japan 2011 from 4.747 to 5.606 μ Hz, for Sumatra earthquake Indonesia 2004 from 3.481 to 5.425 μ Hz (Cordaro, et al 2018). These fundamental frequencies were detected before the earthquake in the areas of Pacific Ocean in the Southern Hemisphere, in the Eurasian (2011) and Philippine (2004) areas in the Northern Hemisphere. Now these significant frequencies are obtained again in different places and time on earth: in Iquique 2014, peaks of 4.611, 4.882, and 5.154 μ Hz and for Illapel 2015, 3.739, 4.630, and 5.520 μ Hz (Figure 4). Up to this point, the rise of these frequencies could be thought as a normal magnetic behavior which a high degree of coincidence. That is why, other methodologies were performed in order to clarify the origin of these frequencies.

In order to avoid bias or technical malfunction, here and after we decided to use different stations that belong to an international network with opensource data (supermag). These stations (OSO and PIL) were the closest to the three earthquakes that had continuous measurements. The time period was 1 year before each earthquake and 1 year after, giving 6 years of combined measurements where the frequency sample was 1 data per minute.

https://doi.org/10.5194/nhess-2020-354
Preprint. Discussion started: 26 November 2020

The first approach was performed by using wavelet analysis at OSO station. Here, in order to avoid normal variations and external perturbation, daily average values were performed by imposing a lower and upper restriction before to apply wavelet analysis. The Figure 5 shows the increase of the frequency range (> 2 μ Hz) 30 days before Maule 2010 earthquake. These frequency activities last up to ~10 days after the earthquake. Despite the abovementioned results, the previous restrictions might be seen as arbitrary. That is why we moved to a stricter, stronger and bias-free methodology.

The definition of magnetic anomalies was performed in sub section 3.5.1. There, the anomalous magnetic variations were defined by using statistical analysis. That is, one variation or peaks will be considered anomalous if it reaches values beyond a certain threshold, threshold defined by the same data. In order to avoid the external perturbations, Dst index and quiet time were considered. This give 6 years of combined data with variations that could be associated to lithosphere or internal. An increase in the frequency range (~1 mHz) before each earthquake was obtained after applying spectrogram analysis (Figure 6). If we look at those periods not close to the earthquake's occurrences, almost no frequency activity was recorded. In addition, these frequencies can not be considered as part of tidal effects because the last one belongs to a different frequency range (~0.01-0.06 mHz) (Casotto and Biscani, 2004, Park et al., 2005). This imply that Maule 2010, Iquique 2014 and Illapel 2015 occurred during very high frequency activity. As the considered data is free of external perturbations, and earthquakes occurrences are within these frequencies' activations, the idea of the existence of lithospherical frequencies related to earthquakes are reinforced.

In order to compare these data with other results, we have performed the count of the daily anomalies. Here, the anomalies behave as a sigmoidal function (Figure 7, 8, 9). In all of the earthquakes was found a dramatic increase in the number of anomalies between 50 to 90 days before each earthquake. This long-term behavior is similar to those found in Nepal 2015 (De Santis et al., 2017), Mexico 2017 (Marchetti and Akhoondzadeh, 2018), Central Italy (Marchetti et al., 2019a), Indonesia 2018 (Marchetti et al., 2019b) or other big earthquakes worldwide (De Santis et al., 2019). Note that the abovementioned studies performed satellite data in contrast with this study that uses ground-based magnetometers and different methodology. Additionally, the station election was following the preparatory phase described by Dobrovolsky et al. (1979). This mean that any magnetic station, close to impending earthquake (~ 1000 km), should detect anomalies or the lithospherical microcracking beneath Earth's surface. The horizontal distance of the preparation phase also agrees to geodetical findings. For example, Bedford et al. (2020) found a preparation phase characterized by a high increase in the strain close to ~1000 km in subduction margin.

By considering the results, the physical mechanism known from the seismo-electromagnetic theory is explained (section 4). This theory explains different empirical observations that indicate a direct relation between magnetic fields and earthquakes in which one the essential group of measurement corresponds to the recording of ultra–low-frequency magnetic signal, mainly close to millihertz and microhertz (Venegas-Aravena et al., 2019, 2020). Here, the anomalies correspond to the manifestation of the crack or micro crack within the lithosphere which allows the flux of electrical current. The temporal evolution of these cracks and its relation to the sigmoidal magnetic anomalies' behavior can be seen in Figure 10. The framework of this theory state that the micro cracks appear as a consequence of the excess of shear stress that cannot be releases by the lithospherical deformation (Venegas-Aravena et al., 2019). Then, frequencies rise and anomalies behavior should be considered as a manifestation of the lithospherical internal collapse at the last stage (preparation stage) of the seismic cycle, when solids cannot hold more strain.

Regarding the mechanism that generates the micro-cracks, we found that the minimum value to define an anomaly was close to 0.2 nT, and this experimental result is in agreement with the theoretical value obtained in Venegas-Aravena et al. (2019), where a ~0.2 nT rise when cracks are created at the semi-brittle ductile regime (depth of 10-20 km).

Let us mention that the frequencies obtained by the Fourier analysis and anomalies are inherent to the lithosphere. The variation of the low frequencies before the earthquake in the magnetic field is due to the ionosphere-atmosphere-lithosphere coupling. We have shown that the frequencies in μHz are related to the Maule earthquake in 2010 (Mw 8.8) (Cordaro et al. 2018). Also, the work of Vallianatos and Tzanis (2003) shows that the magnetic field frequencies are possibly related to earthquake included in a range of at least three orders of magnitude and finally detecting a month before the earthquake in the range of frequencies between 5 -100 *mHz* based on the Ionosphere-Lithosphere-atmosphere coupling.

We also remark that the possibility to predict the future occurrence of these seismic events is not yet possible because the seismological mechanism of seismic movements is not yet precise. However, a correlation does appear to exist between a cumulative number of magnetic anomalies, time-lapse, frequency arise, and the Maule 2010, Iquique 2014, and Illapel 2015 earthquakes. This could be used as a tool to show the behavior of some geophysical variables to indicate plate movements in the future. This condition, based on the increase of low frequencies in the range of $(\mu Hz - mHz)$ suggests that these magnetic variations in the radial component are probably a necessary but not sufficient condition on the Chilean margin. Further investigations on this subject are required.

The next experimental step in this analysis is to gather the measuring instruments of the network (magnetometers, Neutrons, others) and their variables recorded in the lithosphere, ionosphere, magnetosphere, cosmic rays particles,) as neutrons, making a synapse or communication between them, in real time (Learn Machine Method, Others), in order to detect, directions, intensities, start and end of frequencies, magnetic clusters, anomalies, or others, that could allow us to generate a warning prior to a seismic movement.

Acknowledgments

The authors thank Dr. L.A. Raggi (Incas-U.Chile) for their collaboration and support. The fluxgate magnetometer at Putre-Incas Observatories is partially supported by FCFM-University of Chile, and Tarapaca University (Chile). LARC observatory The Chile/Italy Collaboration via U. Chile (Chile), PNRA (ITALY) supports, and INACh partial support. The results presented in this paper rely on data collected at magnetic observatories. We thank the national institutes that support them and INTERMAGNET for promoting high standards of magnetic observatory practice (www.intermagnet.org).. E. G. Cordaro acknowledges Marcela Larenas and Francesca, Beatriz and Enrique for outstanding support to carry out this work.

References

Abad, M., Izquierdo, T., Cáceres, M., Bernárdez, E., Rodriguez-Vidal, J.: Coastal boulder deposit as evidence of an ocean-wide prehistoric tsunami originated on the Atacama Desert coast (northern Chile). Sedimentology 67, 1505–1528, 2020.

Anastasiadis, C., Triantis, D., Stavrakas, I., and Vallianatos, F.: Pressure Stimulated Currents (PSC) in marble samples. Ann. Geophys., 47, 21–28, doi: 10.4401/ag-3255, 2004.

Balasis, G. and Mandea, M.: Can electromagnetic disturbances related to the recent great earthquakes be detected by satellite magnetometers? Tectonophysics, 431, 173–195, doi: 10.1016/j.tecto.2006.05.038, 2007.

Bedford, J.R., Moreno, M., Deng, Z., Oncken, O., Schurr, B., John, T., Báez, J.C. and Bevis, M.: Months-long thousand-kilometre-scale wobbling before great subduction earthquakes. Nature 580, 628–635 (2020), doi: 10.1038/s41586-020-2212-1, 2020.

Blagoveshchensky, D. V., Maltseva, O. A., and Sergeeva, M. A.: Impact of magnetic storms on the global TEC distribution, Ann. Geophys., 36, 1057–1071, https://doi.org/10.5194/angeo-36-1057-2018, 2018.

Bloxham, J., Zatman, S. and Dumberry, M.: The origin of geomagnetic jerks. Nature 420, 65-68 (7 November 2002). doi: 10.1038/nature01134, 2002.

Cartwright-Taylor, A., Vallianatos, F., and Sammonds, P.: Superstatistical view of stress-induced electric current fluctuations in rocks, Physica A, 414, 368–377, 2014.

Carvajal, M., Cisternas, M. and Catalán, P.A.: Source of the 1730 Chilean earthquake from historical records: Implications for the future tsunami hazard on the coast of Metropolitan Chile, J. Geophys. Res. Solid Earth, 122, 3648–3660, doi:10.1002/2017JB014063, 2017.

Casotto, S. and Biscani, F.: A fully analytical approach to the harmonic development of the tide-generating potential accounting for precession, nutation, and perturbations due to figure and planetary terms. AAS Division on Dynamical Astronomy, April 2004, vol. 36(2), 67, 2004.

Chernogor, L.F.: Possible Generation of Quasi-Periodic Magnetic Precursors of Earthquakes. Geomagn. Aeron. 59, 374–382 (2019), doi: 10.1134/S001679321903006X, 2019.

Chulliat, A., Lalanne, X., Gaya-Pique, L.R., Truong, F. and Savary, J.: The new Easter Island magnetic observatory. Proceedings of the XIIIth IAGA Workshop on Geomagnetic Observatory Instruments, Data Acquisition and Processing, edited by J. J. Love, 271 pp., U.S. Geological Survey Open-File Report 2009-1226, 2009.

Contoyiannis, Y., Potirakis, S.M., Eftaxias, K., Hayakawa, M., Schekotov, A.: Intermittent criticality revealed in ULF magnetic fields prior to the 11 March 2011 Tohoku earthquake (Mw = 9). Physica A 452, 19–28, doi: 10.1016/j.physa.2016.01.065, 2016.

Cordaro, E.G., Olivares, E., Gálvez, D., Salazar-Aravena, D., Laroze, D.: New 3He neutron monitor for Chilean osmic-ray observatories from the Altiplanic Zone to the Antarctic zone. Adv. Space Res. 49, 1670, doi: 10.1016/j.asr.2012.03.015, 2012.

Cordaro, E.G., Gálvez, D. and Laroze, D.: Observation of intensity of cosmic rays and daily magnetic shifts near meridian 70° in the South America. Journal of Atmospheric and Solar-Terrestrial Physics. Volume 142, May 2016, Pages 72–82. doi: 10.1016/j.jastp.2016.02.015, 2016.

Cordaro, E.G., Venegas, P. and Laroze, D.: Latitudinal variation Rate of Geomagnetic Cutoff Rigidity in the active Chilean convergent margin. Annales Geophysicae Angeo-2017-176. 2018, doi: 10.5194/angeo-36-275-2018, 2018.

Cordaro, E.G., Venegas-Aravena, P. and Laroze, D.: Variation of geomagnetic cutoff rigidity in the southern hemisphere close to 70°W (South-Atlantic Anomaly and Antarctic zones) in the period 1975-2010, Advances in Space Research, https://doi.org/10.1016/j.asr 2018.12.019, 2019.

De Santis, A., De Franceschi, G., Spogli, L., Perrone, L., Alfonsi, L., Qamili, E., Cianchini, G., Di Giovambattista, R., Salvi, S., Filippi, E., Pavón-Carrasco, F.J., Monna, S., Piscini, A., Battiston, R., Vitale, V., Picozza, P.G., Conti, L., Parrot, M., Pinçon, J.-L., Balasis, G., Tavani, M., Argan, A., Piano, G., Rainone, M.L., Liu, W. and Tao, D.: Geospace perturbations induced by the Earth: The state of the art and future trends. Physics and Chemistry of the Earth, Parts A/B/C, Vol. 85–86, Pages 17-33, doi: 10.1016/j.pce.2015.05.004, 2015.

De Santis, A., Balasis, G., Pavón-Carrasco, F.J. Cianchini G. and Mandea M.: Potential earthquake precursory pattern from space: The 2015 Nepal event as seen by magnetic Swarm satellites. Earth and Planetary Science Letters 461 (2017) 119–126. http://dx.doi.org/10.1016/j.epsl.2016.12.037, 2017.

De Santis, A., Marchetti, D., Spogli, L., Cianchini, G., Pavón-Carrasco, F.J., De Franceschi, G., Di Giovambattista, R.,Perrone, L., Qamili, E., Cesaroni, C., De Santis, A., Ippolito, A., Piscini, A., Campuzano, S.A., Sabbagh, D., Amoruso, L., Carbone, M., Santoro, F., Abbattista, C. and Drimaco, D.: Magnetic Field and Electron Density Data Analysis from Swarm Satellites Searching for Ionospheric Effects by Great Earthquakes: 12 Case Studies from 2014 to 2016. Atmosphere2019 ,10, 371; doi: 10.3390/atmos10070371, 2019.

Diego, P., Storini, M., Parisi, M. and Cordaro, E.: AE index variability during corotating fast solar wind streams. J. Geophys. Res.110, doi:10.1029/2004JA010715, 2005.

Dobrovolsky, I.R., Zubkov, S.I. and Myachkin, V.I.: Estimation of the size of earthquake preparation zones. Pure Appl. Geophys. 117, 1025–1044, doi: 10.1007/BF00876083, 1979.

Fenoglio, M. A., Johnston, M. J. S., and Byedee, J.: Magnetic and electric fields associated with changes in high pore pressure in fault zones: application to the Loma Prieta ULF emissions, J. Geophys. Res., 100, 12951–12958, 1995.

Finlay, C.: Magnetohydrodynamics Waves, Encyclopedia of Geomagnetism and Paleomagnetism, Edited by D. Gubbins and E. Herrero-Berbera. Springer, Netherlands, 2007.

Florios, K., Contopoulos, I., Christofilakis, V., Tatsis, G., Chronopoulos, S., Repapis, C. and Tritakis, V.: Pre-seismic Electromagnetic Perturbations in Two Earthquakes in Northern Greece. Pure Appl. Geophys. 177, 787–799 (2020). https://doi.org/10.1007/s00024-019-02362-6, 2020.

Fraser-Smith, A.C.: Ultralow-frequency magnetic fields preceding large earthquakes, Eos Trans., 2008, vol. 89, no. 23, p. 211, doi: 10.1029/2008EO230007, 2008.

Freund, F.: Toward a unified solid-state theory for pre-earthquake signals, Acta Geophys., 58, 719–766, 2010.

Geller, R.J.: Earthquake prediction: a critical review. Geophysical Journal International, Volume 131, Issue 3, December 1997, Pages 425–450, doi: 10.1111/j.1365-246X.1997.tb06588.x, 1997.

Gjerloev, J. W.: The SuperMAG data processing technique, *J. Geophys. Res.*, 117 A09213, doi: 10.1029/2012JA017683, 2012.

Gubbins, D., Jones, A.L. and Finlay, C.C.: Fall in Earth's magnetic field is erratic. Science 312: 900–902, doi: 10.1126/science.1124855, 2006.

Hayakawa, M. and Molchanov, O.A. (eds.): Seismo Electromagnetics: Lithosphere-Atmosphere-Ionosphere Coupling. TERRAPUB, Tokyo, 2002.

Hayakawa, M., Schekotov, A., Potirakis, S., Eftaxias, K.: Criticality features in ULF magnetic fields prior to the 2011 Tohoku earthquake. Proc. Jpn. Acad. Ser. B, Phys. Biol. Sci. 91, 25–30, doi: 10.2183/pjab.91.25, 2015.

Heirtzler, J.: The future of the South Atlantic Anomaly and implications for radiation damage in space. Journal of Atmospheric and Solar Terrestrial Physics 64: 1701–1708, doi: 10.1016/S1364-6826(02)00120-7, 2002.

Herbst, K., Kopp, A., Heber, B.: Influence of the terrestrial magnetic field geometry on the Cutoff Rigidity of cosmic ray particles. Ann. Geophys. 31, 1637–1643, doi: 10.5194/angeo-31-1637-2013, 2013.

Herman, M.W., Furlong, K.P., Hayes, G.P. and Benz, H.M.: Foreshock triggering of the 1 April 2014 Mw 8.2 Iquique, Chile, earthquake, Earth and Planetary Science Letters, Volume 447, 1 August 2016, Pages 119-129, doi: 10.1016/j.epsl.2016.04.020, 2016.

Hitchmn, A.P, Lilley, F.E.M. and Campbell, W.H.: The quiet daily variation in the total magnetic field: global curves. Geophysical Research Letters, VOL. 25, NO. 11, p2007-2010, June 1, 1998, doi: 10.1029/98GL51332, 1998.

Ippolito, A., Perrone. L., De Santis, A. and Sabbagh D.: Ionosonde Data Analysis in Relation to the 2016 Central Italian Earthquakes. Geosciences 2020, 10, 354; doi:10.3390/geosciences10090354, 2020.

Jordan, T., Chen, Y., Gasparini, P., Madariaga, R., Main, I., Marzocchi, W., Papadopoulos, G., Sobolev, G., Yamaoka, K. and Zschau, J.: Operational earthquake forecasting. State of Knowledge and Guidelines for Utilization. Annals of Geophysics, 54(4), doi: 10.4401/ag-5350, 2011.

Kanamori, H.: The Energy Release in Great Earthquakes, J. Geophys. Res., 82(20), 2981–2987, 1977.

Karakeliana, D., Klemperera, S. L., Fraser-Smith, A. C., and Thompson, G. A.: Ultra-low frequency electromagnetic measurements associated with the 1998 Mw 5.1 San Juan Bautista, California earthquake and implications for mechanisms of electromagnetic earthquake precursors, Tectonophysics, 359, 65–79, 2002.

Kivelson, M, G. and Russell, C.T.: Introduction to Space Physics. Cambridge, Cambridge University Press, doi: 10.1017/9781139878296, 1995.

Kulsrud, R.: Plasma Physics for Astrophysics. Princeton University Press, U.S.A. Lanza, R., Meloni, A., 2006. The Earth's Magnetism – An Introduction for Geologists. Springer, Würzburg.

Lassak, T., McNamara, A., Garnero, E., and Zhong, S.: Core–mantle boundary topography as a possible constraint on lower mantle chemistry and dynamics. Earth and Planetary Science Letters, Vol. 289, Issues 1–2, 15 January 2010, Pages 232-241, doi: 10.1016/j.epsl.2009.11.012, 2010.

Lazarian, A., Eyink, G.L., Jafari, A., Kowal, G., Li, H., Xu, S. and Vishniac, E.T.: 3D turbulent reconnection: Theory, tests, and astrophysical implications. Physics of Plasmas 27, 012305 (2020); https://doi.org/10.1063/1.5110603, 2020.

Li, Z., Zhang, X., Wei, Y. and Ali, M.: Experimental Study of Electric Potential Response Characteristics of Different Lithological Samples Subject to Uniaxial Loading. Rock Mech Rock Eng (2020). https://doi.org/10.1007/s00603-020-02276-z, 2020.

Liu, J.Y.: Earthquake precursors observed in the ionospheric F-region. In Electromagnetic Phenomena Associated with Earthquakes (ed. Hayakawa, M.). Transworld Research Network, Trivandrum, India, pp. 187–204, 2009.

Ma, L., Zhao, J., and Ni, B.: A Zener-Stroh crack interacting with an edge dislocation, Theoretical and Applied Mechanics Letters, 2, 021003, https://doi.org/10.1063/2.1102103, 2011.

Marchetti, D. and Akhoondzadeh, M.: Analysis of Swarm satellites data showing seismo-ionospheric anomalies around the time of the strong Mexico (Mw = 8.2) earthquake of 08 September 2017. Advances in Space Research, Vol. 62, Issue 3, 1 August 2018, Pages 614-623, doi: 10.1016/j.asr.2018.04.043, 2018.

Marchetti, D., De Santis, A., D'Arcangelo, S., Poggio, F., Piscini, A., Campuzano, S.A. and De Carvalho, W.V.J.O.: Pre-earthquake chain processes detected from ground to satellite altitude inpreparation of the 2016–2017 seismic sequence in Central Italy. Remote Sensing of Environment. Volume 229, August 2019, Pages 93-99, doi: 10.1016/j.rse.2019.04.033, 2019a.

Marchetti, D., Santis, A. D., Shen, X., Campuzano, S. A., Perrone, L., Piscini, A., Di Giovambattista, R., Jin, S., Ippolito, A., Cianchini, G., Cesaroni C., Sabbagh, D., Spogli, L. Zhima, Z. and Huang, J.: Possible Lithosphere-Atmosphere-Ionosphere Coupling effects prior to the 2018 Mw=7.5 Indonesia earthquake from seismic, atmospheric and ionospheric data. Journal of Asian Earth Sciences, 104097. doi: 10.1016/j.jseaes.2019.104097, 2019b.

McFadden, P.L. and Merrill, R.T.: Geomagnetic Field, Asymmetries, Encyclopedia of Geomagnetism and Paleomagnetism, Edited by D. Gubbins and E. Herrero-Berbera. Springer, Netherlands, 2007.

Molchanov, O.A. and Hayakawa, M.: SeismoElectromagnetics and Related Phenomena: History and Latest Results. TERRAPUB, Tokyo, 2008.

Moldwin, M.: An introduction to space weather. Cambridge University Press. doi: 10.1017/CBO9780511801365, 2008.

Oikonomou, C., Haralambous, H. and Muslim, B.: Investigation of ionospheric precursors related to deep and intermediate earthquakes based on spectral and statistical analysis. Advances in Space Research 59 (2017) 587–602 doi: 10.1016/j.asr.2016.10.026, 2017.

Olson, P., Christensen, U.R. and Glatzmaier, G.A.: Numerical modeling of the geodynamo: mechanisms of field generation and equilibration, J. geophys. Res., 104, 10 383–10 404, doi: 10.1029/1999JB900013, 1999.

Olson, P.: Core Dynamics: An Introduction and Overview, Treatise on Geophysics (Second Edition) 2015, Pages 1–25 Reference Module in Earth Systems and Environmental Sciences Volume 8: Core Dynamics doi:10.1016/B978-0-444-53802-4.00137-8, 2015.

Oppenheim, A.V., Schafer, R.W., and Buck, J. R.: Discrete-Time Signal Processing. 2nd Ed. Upper Saddle River, NJ: Prentice Hall, 1999.

Park, J., Song, T.-R. A., Tromp, J., Okal, E., Stein, S., Roult, G., Clevede, E., Laske, G., Kanamori, H., Davis, P., Berger, J., Braitenberg, C., Van Camp, M., Lei, X., Sun, H., Xu, H. and Rosat, S.: Earth's Free Oscillations Excited by the 26 December 2004 Sumatra-Andaman Earthquake. Science 20 May 2005: Vol. 308, Issue 5725, pp. 1139-1144. DOI: 10.1126/science.1112305, 2005.

Pedrera, A., Galindo-Zaldívar, J., Ruiz-Constán, A., Bohoyo, F., Torres-Carbonell, P., Ruano, P., Maestro, A. and González-Castillo, L.: The last major earthquakes along the Magallanes-Fagnano fault system recorded by disturbed trees (Tierra del Fuego, South America). Terra Nova 26, 448–453, doi: 10.1111/ter.12119 2014.

Pomerantz, M.A.: Cosmic Rays. Published by The Commission on College Physics. Rd. Van Nostrand Reinhold Company, 1971.

Potirakis, S., Eftaxias, K., Schekotov, A., Yamaguchi, H. and Hayakawa, M.: Criticality features in ultra-low frequency magnetic fields prior to the 2013 M6.3 Kobe earthquake. Ann. Geophys. Vol. 59, No 3, doi: 10.4401/ag-6863, 2016.

Potirakis, S.M., Asano, T. and Hayakawa, M.: Criticality Analysis of the Lower Ionosphere Perturbations Prior to the 2016 Kumamoto (Japan) Earthquakes as Based on VLF Electromagnetic Wave Propagation Data Observed at Multiple Stations. Entropy 2018, 20, 199; doi: 10.3390/e20030199, 2018.

Priest, E.R., Forbes, T.: Magnetic Reconnection: Mhd Theory and Applications, Cambridge University Press, New York, 2000.

Prutkin, I.: Gravitational and magnetic models of the core–mantle boundary and their correlation. Journal of Geodynamics, Vol 45, Issues 2–3, March 2008, Pages 146-153, doi: 10.1016/j.jog.2007.09.001, 2008.

Pulinets, S. and Boyarchuk, K: Ionospheric Precursors of Earthquakes. Springer, Berlin, doi: 10.1007/b137616, 2004.

Rabiner, L.R. and Schafer, R.W.: Digital Processing of Speech Signals. The Journal of the Acoustical Society of America 67, 1406 (1980); doi: 10.1121/1.384160, 1980.

Russel, C.T., Zhou, X.W., Chi, P.J., Kawano, H., Moore, T.E., Peterson, W.K., Cladis, J.B. and Singer, H.J.: Sudden compression of the outer magnetosphere associated with an ionospheric mass ejection. Geophys. Res. Lett. 26,2343, doi:10.1029/1999GL900455, 1999.

Sarson, G.R.: Dynamo Waves, Encyclopedia of Geomagnetism and Paleomagnetism, Edited by D. Gubbins and E. Herrero-Berbera. Springer, Netherlands, 2007.

Satake, K., Heidarzadeh, M., Quiroz, M. and Cienfuegos, R.: History and features of trans-oceanic tsunamis and implications for paleo-tsunami studies. Earth-Science Reviews, Volume 202, March 2020, 103112, doi: 10.1016/j.earscirev.2020.103112, 2020.

Scoville, J., Heraud, J. and Freund, F.: Pre-earthquake magnetic pulses. Nat. Hazards Earth Syst. Sci., 15, 1873–1880, 2015. doi:10.5194/nhess-15-1873-2015, 2015.

Hough, S. E.: Predicting the Unpredictable: The Tumultuous Science of Earthquake Prediction, Vol. 272, Princeton: Princeton University Press. doi: 10.1515/9781400883547, 2010.

https://doi.org/10.5194/nhess-2020-354
Preprint. Discussion started: 26 November 2020

Natural Hazards and Earth System Sciences
Open Access
EGU
Discussions

Shea, M.A. and Smart, D.F.: Vertical cutoff rigidities for cosmic ray stations since 1955. Proc. 27th Int. Cosmic Ray Conf., Hamburg, 10, 4063–4066, 2001.

Siebert, M. and Meyer, J.: Geomagnetic activity indices. In: Dieminger W, Hartman GK, and Leitinger R (eds.) The Upper Atmosphere, pp. 887–911. Berlin Heidelberg/New York: Springer, 1996.

Silva, R. P., Sobral, J. H. A., Koga, D., and Souza, J. R.: Evidence of prompt penetration electric fields during HILDCAA events, Ann. Geophys., 35, 1165–1176, https://doi.org/10.5194/angeo-35-1165-2017, 2017.

Simmons, N.A., Forte, A.M., Boschi, L. and Grand, S.P.: Gypsum: A joint tomographic model of mantle density and seismic wave speeds. Journal of Geophysical Research (2010) 115: B12310. http://dx.doi.org/10.1029/2010JB007631, 2010.

Smart, D.F., Shea, M.A., Flückiger, E.O.: Magnetospheric models and trajectory computations. Space Sci. Rev. 93 (1), 305–333 2000.

Smart, D.F., Shea, M.A.: Geomagnetic Cutoff Rigidity computer program Theory, Software Description and Example. Final Report, Grant NAG5-8009. Center for Space Plasmas and Aeronomic Research, the University of Alabama in Huntsville, 2001.

Smart, D.F. and Shea, M.A.: A review of geomagnetic cutoff rigidities for earth-orbiting spacecraft. *Advances in Space Research* 36 (2005) pp. 2012–2020. doi: 10.1016/j.asr.2004.09.015, 2005.

Soldati, G., Boschi, L., and Forte, A.M.: Tomography of core–mantle boundary and lowermost mantle coupled by geodynamics. Geophysical Journal International (2012) 189: 730–746, doi: 10.1111/j.1365-246X.2012.05413.x, 2012.

Soloviev, A., Chulliat, A., Bogoutdinov, S., Gvishiani, A., Agayan, S., Peltier, A. and Heumez, B.: Automated recognition of spikes in 1 Hz data recorded at the Easter Island magnetic observatory. Earth Planets Space, 64, 743–752, doi: 10.5047/eps.2012.03.004, 2012.

Stewart, D.N., Busse, F.H., Whaler, K. and Gubbins, D.: Geomagnetism Earth rotation and the electrical conductivity of the lower mantle. Phys. Earth Planet. Inter., 92, 199-214), doi: 10.1016/0031-9201(95)03035-4, 1995.

Storini, M., Shea, M.A., Smart, D.F. and Cordaro, E.G.: Cutoff Variability for the Antarctic Laboratory for Cosmic Rays (LARC: 1955-1995). 26th International Cosmic Ray Conference. SH.3.6.30 .7 1999. 402, 1999.

Stavrakas, I., Triantis, D., Agioutantis, Z., Maurigiannakis, S., Saltas, V., Vallianatos, F., and Clarke, M.: Pressure stimulated currents in rocks and their correlation with mechanical properties, Nat. Hazards Earth Syst. Sci., 4, 563–567, https://doi.org/10.5194/nhess-4-563-2004, 2004.

Stavrakas, I., Kourkoulis, S., and Triantis, D.: Damage evolution in marble under uniaxial compression monitored by Pressure Stimulated Currents and Acoustic Emissions. Frattura Ed Integrità Strutturale, 13(50), 573-583. https://doi.org/10.3221/IGF-ESIS.50.48, 2019.

Tarduno, J.A., Watkeys, M.K., Huffman, T.N., Cottrell, R.D., Blackman, E.G., Wendt, A., Scribner, C.A. and Wagner, C.L.: Antiquity of the South Atlantic Anomaly and evidence for top-down control on the geodynamo. Nat Commun 6, 7865, doi:10.1038/ncomms8865, 2015.

Torrence, C. and Compo, G.P.: A Practical Guide to Wavelet Analysis. Bulletin of the American Meteorological Society, vol. 79, Issue 1, pp.61-78, doi: 10.1175/1520-0477(1998)079<0061:APGTWA>2.0.CO;2, 1998.

Triantis, D., Anastasiadis, C. and Stavrakas, I.: The correlation of electrical charge with strain on stressed rock samples, Nat. Hazards Earth Syst. Sci., 8, 1243–1248, https://doi.org/10.5194/nhess-8-1243-2008, 2008.

Tsyganenko, N.A.: A model of the near magnetosphere with a dawn-dusk asymmetry 1. Mathematical structure. J. Geophys. Res. 107 (A8), 1179, doi: 10.1029/2001JA000219, SMP12-1-17, 2002a.

Tsyganenko, N.A.: A model of the near magnetosphere with a dawn-dusk asymmetry 2: parametrization and fitting to observation. J. Geophys. Res. 107 (A8), 1176, doi:10.1029/2001JA000219, 2002b.

Tzanis, A. and Vallianatos, F.: A physical model of electrical earthquake precursors due to crack propagation and the motion of charged edge dislocations. Seismo Electromagnetics (Lithosphere–Atmosphere–Ionosphere-Coupling), TerraPub, 2002, pp. 117–130, 2002.

Utada, H., Shimizu, H., Ogawa, T., Maeda, T., Furumura, T., Yamamoto, T., Yamazaki, N., Yoshitake, Y., and Nagamachi, S.: Geomagnetic field changes in response to the 2011 off the Pacific Coast of Tohoku earthquake and tsunami, Earth Planet. Sc. Lett., 311, 11–27, https://doi.org/10.1016/j.epsl.2011.09.036, 2011.

Vallianatos, F. and Tzanis, A.: On the nature, scaling and spectral properties of pre-seismic ULF signals. Natural Hazards and Earth System Sciences (2003) 3: 237–242. European Geosciences Union, doi: 10.5194/nhess-3-237-2003, 2003.

Varotsos, P., Eftaxias, K., Lazaridou, M., Antonopoulos, G., Makris, J. and Poliyiannakis, J.: Summary of the five principles suggested by Varotsos et al. [1996] and the additional questions raised in this debate. Geophysical Research Letter. Volume23, Issue 11, 27 May 1996, p1449-1452, doi: 10.1029/96GL01437, 1996.

Varotsos, P.A.: The Physics of Seismic Electric Signals. Journal of atmospheric electricity, 33(1), 53-68, TERRAPUB, Tokyo, 2005.

Venegas-Aravena, P., Cordaro E.G. and Laroze. D.: A review and upgrade of the lithospheric dynamics in context of the seismo-electromagnetic theory. Natural Hazards Earth System Sciences. 119, 1- 13, doi: 10.5194/nhess- 19-1-2019, 2019.

Venegas-Aravena, P., Cordaro E.G. and Laroze. D.: The spatial–temporal total friction coefficient of the fault viewed from the perspective of seismo-electromagnetic theory. Nat. Hazards Earth Syst. Sci., 20, 1485–1496, doi: 10.5194/nhess-20-1485-2020, 2020.

Vezzoli, L. and Acoocella, V.: Easter Island, SE Pacific: An end-member type of hotspot volcanism. Geological Society of American Bulletin, May/june 2009, V. 121; no 5/6, p 869-886, doi:10.1130/B26470.1, 2009.

Vigny, C., Socquet, A., Peyrat, S., Ruegg, J.-C., Metois, M., Madariaga, R., Morvan, S.,Lancieri, M., Lacassin, R., Campos, J., Carrizo, D., Bejar-Pizarro, M., Barrientos, S., Armijo, R., Aranda, C., Valderas-Bermejo, M.-C., Ortega, I., Bondoux, F., Baize, S.,Lyon-Caen, H., Pavez, A., Vilotte, J. P., Bevis, M., Brooks, B., Smalley, R., Parra, H., Baez, J.-C., Blanco, M., Cimbaro, S., and Kendrick, E.: The 2010 Mw 8.8 Maule Megathrust Earthquake of Central Chile, monitored by GPS, Science, 332, 1417–1421, 2011.

Villalobos, C.U., Bravo, M.A., Ovalle, E.M. and Foppiano, A.J.: Ionospheric characteristics prior to the greatest earthquake in recorded history. Advances in Space Research, 57 (2016) 1345–1359, doi: 10.1016/j.asr.2015.09.015, 2016.

Vogel, E. E., Brevis, F. G., Pastén, D., Muñoz, V., Miranda, R. A., and Chian, A. C.-L.: Measuring the seismic risk along the Nazca–South American subduction front: Shannon entropy and mutability, Nat. Hazards Earth Syst. Sci., 20, 2943–2960, https://doi.org/10.5194/nhess-20-2943-2020, 2020.

Yamanaka, C., Matsumoto, H. and Asahara, H.: Preseismic Electromagnetic Phenomena. IEEJ Transactions on Fundamentals and Materials. Special Issue Paper, 2016 Volume 136 Issue 5 Pages 310-314, doi: 10.1541/ieejfms.136.310, 2016.

Yeeram, T.: The solar wind-magnetosphere coupling and daytime disturbance electric fields in equatorial ionosphere during consecutive recurrent geomagnetic storms. Journal of Atmospheric and Solar-Terrestrial Physics, Volume 187, June 2019, Pages 40-52, doi: 10.1016/j.jastp.2019.03.004, 2019.

Yoshida, M.: Core–mantle boundary topography estimated from numerical simulations of instantaneous mantle flow. Geochemistry, Geophysics, Geosystems, Vol. 9, No. 7, 2 July 2008, doi: 10.1029/2008GC002008, 2008.

Zhang, Y., Zhang, G., Hetland, E.A., Shan, X., Wen, S. and Zuo, R.: Coseismic Fault Slip of the September 16, 2015 Mw 8.3 Illapel, Chile Earthquake Estimated from InSAR Data. In: Braitenberg C., Rabinovich A. (eds) The Chile-2015 (Illapel) Earthquake and Tsunami. Pageoph Topical Volumes. Birkhäuser, Cham, doi: 10.1007/978-3-319-57822-4_7, 2017.

Figure Captions

Figure 1: Left side: Latitudinal effect of the Geomagnetic cutoff rigidity projected over the Chilean convergent margin close to the 70° W meridian. The pink solid lines indicate the edges of tectonic plates. Nazca Plate from 18° North to 45° degrees latitudinal, The South American Continent on the South American Plate. The 45 ° to 79° the Antarctic Plate. The black lines indicate coast line. In blue the iso values of magnetic intensity due SAMA proximity. The symbols indicate stations location. Right: History of Chilean earthquakes.

Figure 2: The Kp magnetic activity index for the periods prior to the Maule 2010 (top), Iquique 2014 (middle) and Illapel 2015 (bottom) earthquakes. [spidr NOAA] [WDCFG Kyoto University] .

Figure 3: Vertical Component B_z as a function of time at Putre and IPM stations. a) Maule 2010 at the Putre station, b) Iquique 2014 at the Putre station, c) Iquique 2014 at the Easter Island station and d) Illapel 2015 at Easter island station. Trends changes has been observed in the four cases.

Figure 4: a) Fast Fourier Transformation (FFT) of the second derivative B_z component at Putre station for different events: Maule 2010 and Iquique 2014. The rise of frequencies in the range of micro Hz are compared to the FFT of the second derivative at IPM station for Illapel 2015. b) FFT every 15 days for Iquique 2015 at the Putre magnetometer. c) FFT every 8 days for Illapel 2015 at the Easter Island magnetometer.

Figure 5: Wavelet for Bz at OSO station is shown. This graph is obtained by restricting the peaks considered in a band and daily average values during 2 years of measurements. Wavelet spectrum shows an increase prior and after Maule Earthquake. Unlike the spectrogram method where it is enough to consider the anomalous peaks on a threshold, wavelet analysis is more complex to calibrate than spectrogram analysis (upper limit).

Figure 6: Spectrograms analysis of vertical magnetic components after the external influence is filtered. a) The rise of a range of frequencies (1-2.5 mHz) appear prior and after the Maule 2010 earthquake (OSO station). The actives frequencies last less than 3 months. b) The rise of similar frequencies appears prior the Iquique 2014 earthquake in the vertical component of PIL station. This frequency activity las more than five months. c) The solar events were intense during September 2015. Nevertheless, it can be seen an increase in the spectrum since August 2015. This frequency activity last close to 3 months. Three earthquakes hit when exist the rise of ultra-low frequencies (mHz)

Figure 7: Accumulated magnetic anomalies of B_z and a lineal interpolation in the period during two years starting in 29 February 2009. The data were taken at OSO Station. Close to the Main earthquake, the linear trend breaks and the number of anomalies increase. Other important seismic events hit near the stations during the last period. Nevertheless, it is not clear that the anomaly increases are due these specific events.

Figure 8: Variation of the accumulated diary of magnetic anomalies of B_z during two years close to the three earthquakes: (a) Maule, (b) Iquique and (c) Illapel. The data were taken at OSO station (a) and PIL station (b & c), respectively. Is clear that the sigmoidal shape is similar in all of the earthquakes. This mean that these stations recorded a dramatic increase in the number of magnetic anomalies between 50 to 90 days prior each earthquake.

Figure 9: (Upper panel) Accumulated Diary of magnetic anomalies during two years, in component Y from Apr 1 to Oct 15, 2017 in Mexico Earthquake Sep 8, 2017 Mw8.2. (Lower panel) Residual behavior of Mexico Earthquake. The data is open source and were taken from swarm project (ftp://swarm-diss.eo.esa.int/). Methodology was developed by Marchetti and Akhoondzadeh (2018).

Figure 10: Schematic representation of the seimo-electromagnetic theory. The anomalies generation are owing the creation of several microcracks. The number of cracks increase because the internal collapse of the lithosphere when a non-constant uniaxial stress is applied.

Table Captions

Table 1: The main characteristics for the detector of Chilean network Cosmic Rays and Geomagnetic Observatories as location, altitude, and atmospheric deep, type of detectors.

Table 2: The maximum radius where the ionosphere-lithosphere-atmosphere coupling may affect magnetic measurements to each earthquake studied at the station of Putre and IPM. (Dobrovolsky et al., 1979, Pulinets and Boyarchuk, 2004). The Preparation area or Dobrovolsky area is defined by the radius $r = 10^{0.43M}$, where M is the earthquake magnitude. This table shos that Putre and IPM stations are within the earthquake preparation stage for Maule, Iquique and Illapel.

Figures

https://doi.org/10.5194/nhess-2020-354
Preprint. Discussion started: 26 November 2020

Natural Hazards and Earth System Sciences
Open Access
Discussions

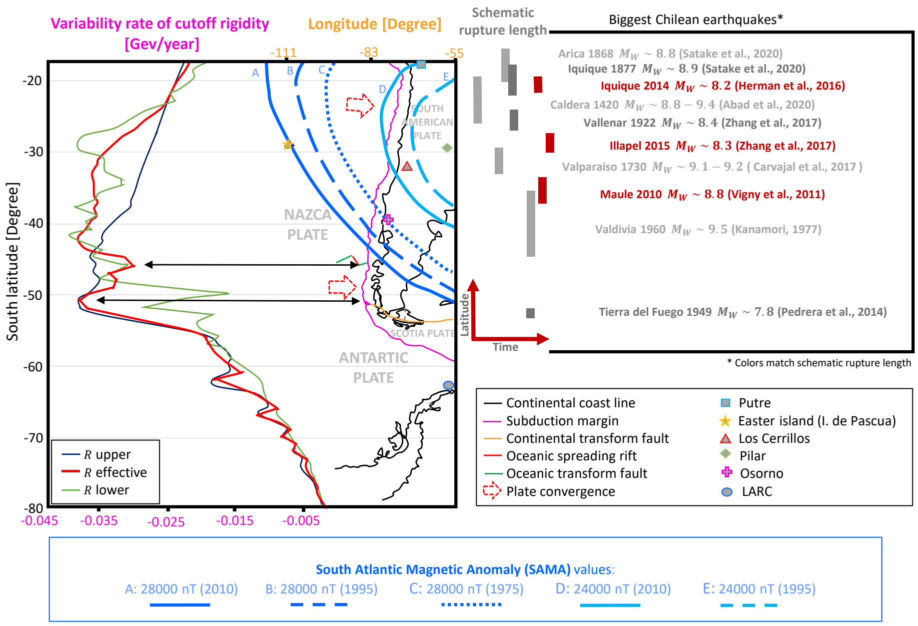

Figure 1

https://doi.org/10.5194/nhess-2020-354
Preprint. Discussion started: 26 November 2020

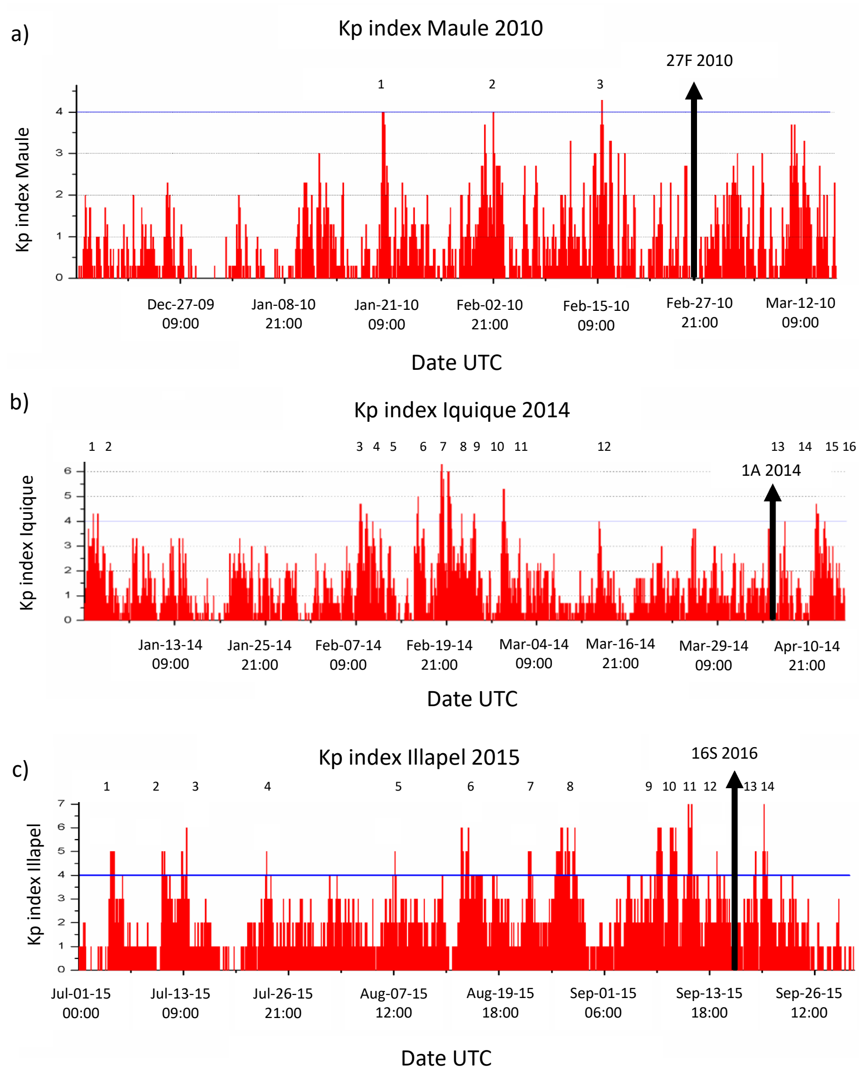

Figure 2 a,b,c

https://doi.org/10.5194/nhess-2020-354
Preprint. Discussion started: 26 November 2020

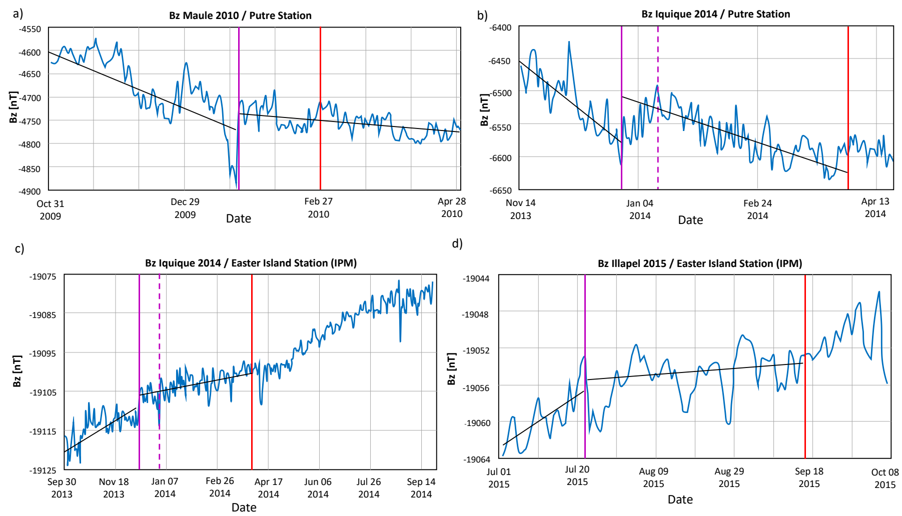

Figure 3 a, b, c, d

https://doi.org/10.5194/nhess-2020-354
Preprint. Discussion started: 26 November 2020

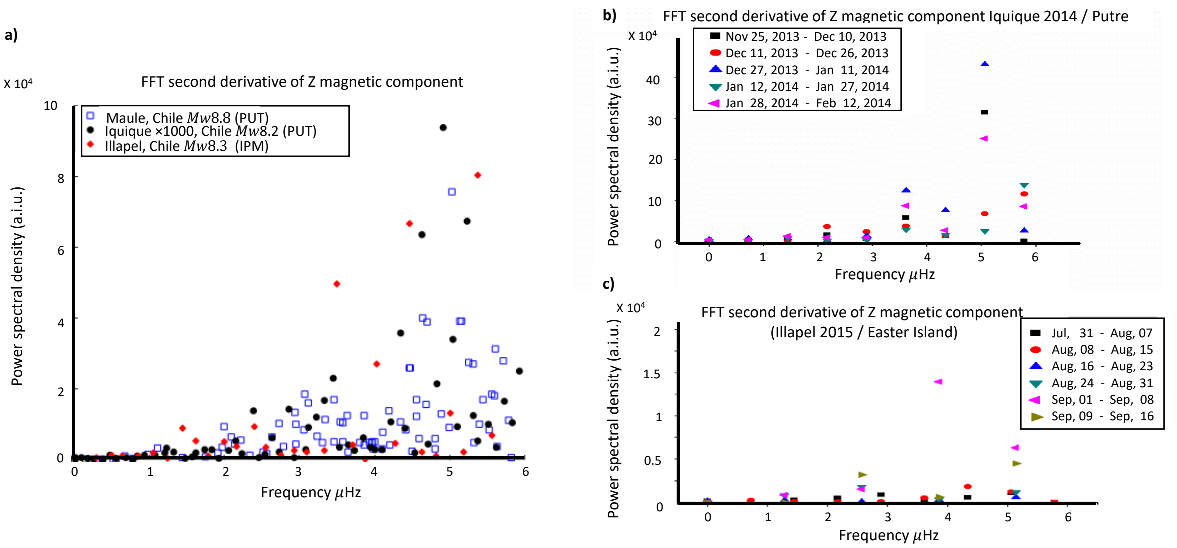

Figure 4 a,b,c

https://doi.org/10.5194/nhess-2020-354
Preprint. Discussion started: 26 November 2020

Natural Hazards and Earth System Sciences Discussions

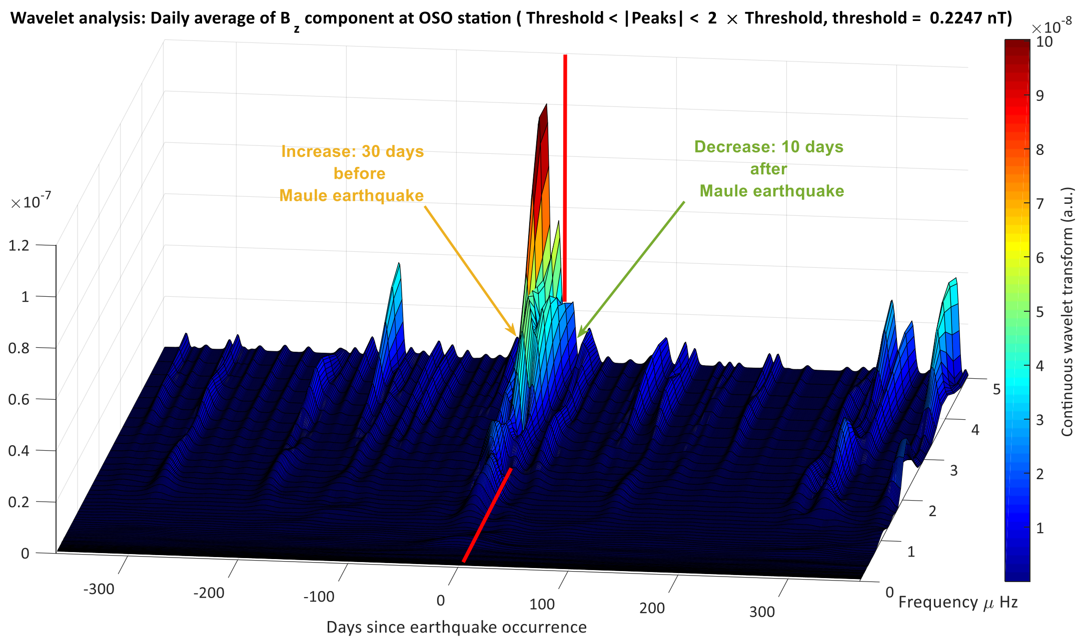

1 **Figure 5**

https://doi.org/10.5194/nhess-2020-354
Preprint. Discussion started: 26 November 2020

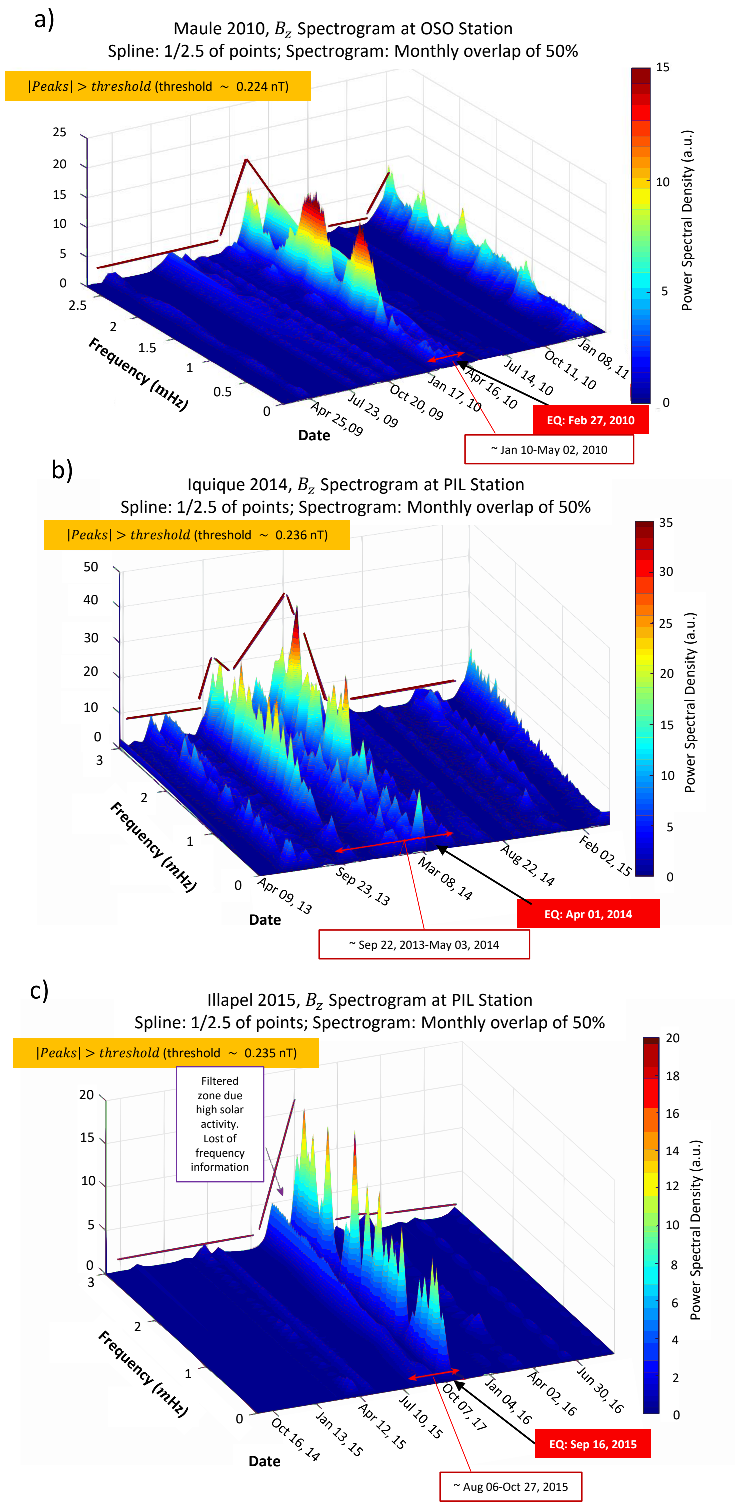

https://doi.org/10.5194/nhess-2020-354
Preprint. Discussion started: 26 November 2020

Natural Hazards and Earth System Sciences
Open Access
Discussions

Figure 6

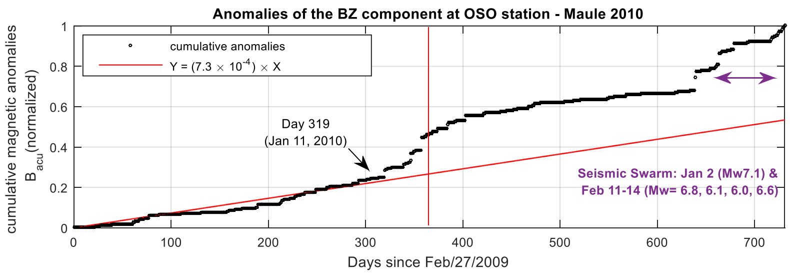

Figure 7

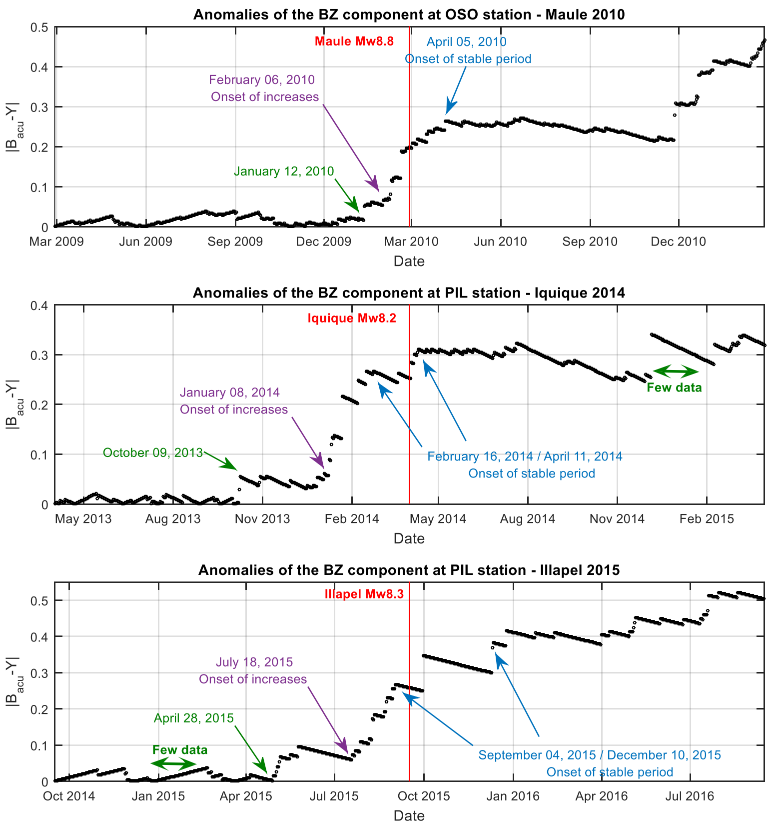
Anomalies of the BZ component at OSO station - Maule 2010
Maule Mw8.8
April 05, 2010
Onset of stable period
February 06, 2010
Onset of increases
January 12, 2010
|B_acu -Y|
Mar 2009
Jun 2009
Sep 2009
Dec 2009
Mar 2010
Jun 2010
Sep 2010
Dec 2010
Date
Anomalies of the BZ component at PIL station - Iquique 2014
Iquique Mw8.2
January 08, 2014
Onset of increases
October 09, 2013
February 16, 2014 / April 11, 2014
Onset of stable period
Few data
|B_acu -Y|
May 2013
Aug 2013
Nov 2013
Feb 2014
May 2014
Aug 2014
Nov 2014
Feb 2015
Date
Anomalies of the BZ component at PIL station - Illapel 2015
Illapel Mw8.3
July 18, 2015
Onset of increases
April 28, 2015
Few data
September 04, 2015 / December 10, 2015
Onset of stable period
|B_acu -Y|
Oct 2014
Jan 2015
Apr 2015
Jul 2015
Oct 2015
Jan 2016
Apr 2016
Jul 2016
Date

Figure 8

https://doi.org/10.5194/nhess-2020-354
Preprint. Discussion started: 26 November 2020

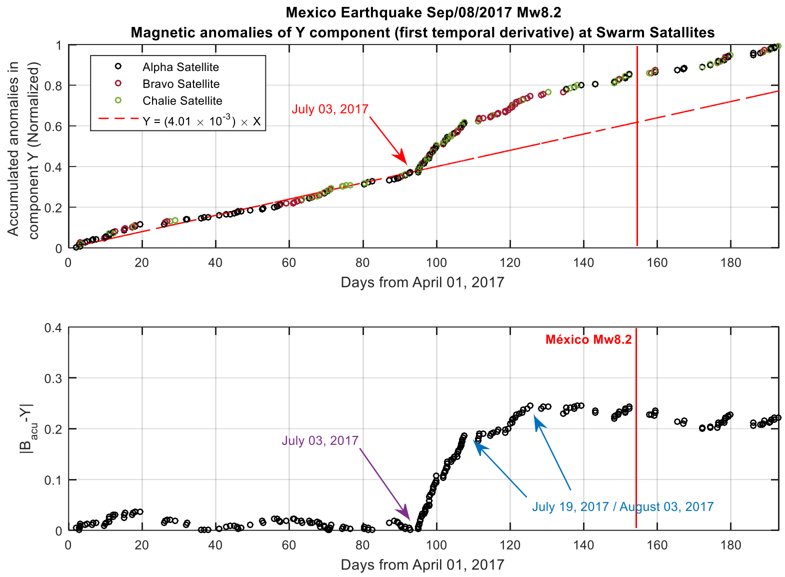

Figure 9

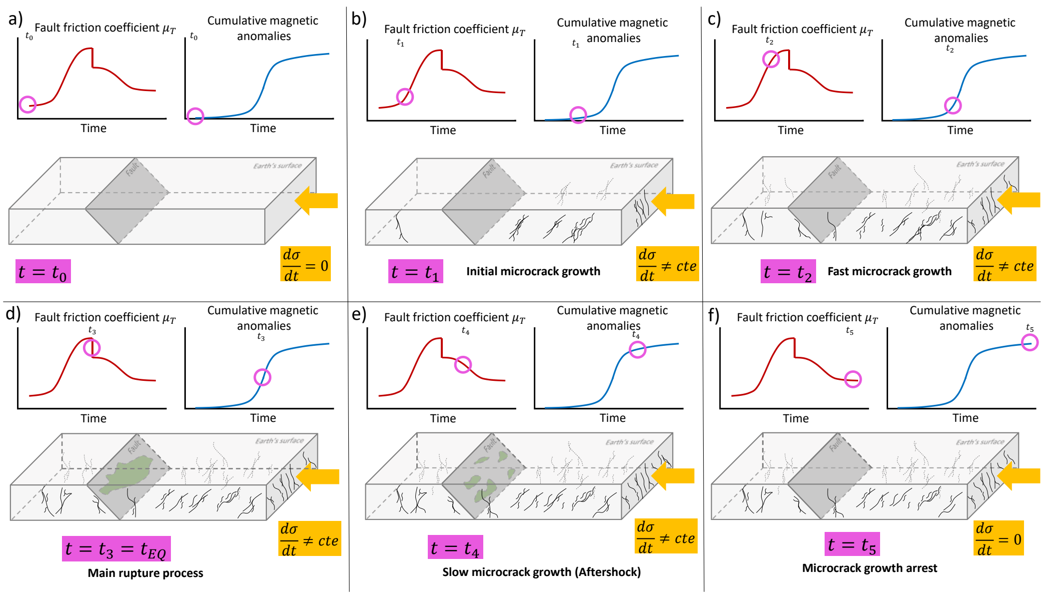

Figure 10

https://doi.org/10.5194/nhess-2020-354
Preprint. Discussion started: 26 November 2020

Observatory	Location	Geographical coordinate	Altitude [m.a.s.l]	Atmospheric Deep [g/cm2]	Instruments	Time
PUTRE (PUT)	Andes Mountain, Chile	18°11´47.8 “ S. 69°33´10.9” W	3.600	666	Magnetometer, UCLA-Vectorial-Flux Gate. Muon telescope, 3 channels. Neutron monitor IGY, 3 channels,He 3. UTC by GPS receiver.	2003-2017
Los Cerrillos (OLC)	Santiago de Chile, Chile	33°29´42.2” S. 70°42´59.81 W	570	955	Magnetometer, UCLA-Vectorial-Flux Gate. Multi-dirctional muon telescope, 7 channels. Neutron monitor 6NM64, 3 channels, BF-3. UTC by GPS receiver.	1958-2017
LARC	King George Island, Antarctic	62°12´9”S. 58°57´42¨ W	40	980	Magnetometer, UCLA-Vectorial-Flux Gate. Neutron monitor 6NM64 - BF-3BF-3. 6 channels. Neutron monitor 3NM64 – He-3. 3 channels, Neutron monitor 3NM64 – He-3.[Flux meter] 3 channels. UTC by GPS receiver.	1990-2017

Table 1

Event	Magnitude [Mw]	Radius r [km]	Station Distance from earthquake [km]
Maule 2010	8.8	~6100	Putre ~ 2030
Iquique 2014	8.2	~3360	Putre ~ 300
Illapel 2015	8.3	~3700	IPM ~ 3700

Table 2